Kramer, W., Drutsa, V., Jansen, H. W., Kramer, B., Pflugfelder, M., & Fritz, H.-J. (1984) *Nucleic Acids Res. 12*, 9441–9456.
Matthews, D. A., Alden, R. A., Freer, S. T., Xuong, N., & Kraut, J. (1979) *J. Biol. Chem. 254*, 4144–4151.
Matthews, D. A., Bolin, J. T., Burridge, J. M., Filman, D. J., Volz, K. W., Kaufman, B. T., Beddell, C. R., Champness, J. N., Stammers, D. K., & Kraut, J. (1985) *J. Biol. Chem. 260*, 381–391.
Roberts, G. C. K., Feeney, J., Burgen, A. S. V., & Daluge, S. (1981) *FEBS Lett. 131*, 85–88.
Searle, M. S., Forster, M. J., Birdsall, B., Roberts, G. C. K., Feeney, J., Kompis, I., & Geddes, A. J. (1988) *Proc. Natl. Acad. Sci. U.S.A. 85*, 3787–3791.
Stone, S. R., & Morrison, J. F. (1984) *Biochemistry 23*, 2753–2758.
Thomson, J. W., Roberts, G. C. K., & Burgen, A. S. V. (1980) *Biochem. J. 187*, 501–506.
Villafranca, J. E., Howell, E. E., Voet, D. H., Stroebel, M. S., Ogden, R. C., Abelson, J. N., & Kraut, J. (1983) *Science (Washington, D.C.) 222*, 782–788.
Wyeth, P., Gronenborn, A., Birdsall, B., Roberts, G. C. K., Feeney, J., & Burgen, A. S. V. (1980) *Biochemistry 19*, 2608–2615.

Protein Dynamics from Chemical Shift and Dipolar Rotational Spin-Echo ^{15}N NMR†

Joel R. Garbow
Monsanto Company, Life Sciences NMR Center, Chesterfield, Missouri 63198
Gary S. Jacob
Department of Molecular and Cell Biology, G. D. Searle & Company, St. Louis, Missouri 63198
E. O. Stejskal
Department of Chemistry, North Carolina State University, Raleigh, North Carolina 27695
Jacob Schaefer*
Department of Chemistry, Washington University, St. Louis, Missouri 63130
Received August 3, 1988

ABSTRACT: The partial collapse of dipolar and chemical shift tensors for peptide NH and for the amide NH at cross-link sites in cell wall peptidoglycan, of intact lyophilized cells of *Aerococcus viridans*, indicates NH vector root-mean-square fluctuations of 23°. This result is consistent with the local mobility calculated in typical picosecond regime computer simulations of protein dynamics in the solid state. The experimental root-mean-square angular fluctuations for both types of NH vectors increase to 37° for viable wet cells at 10 °C. The similarity in mobilities for both general protein and cell wall peptidoglycan suggests that one additional motion in wet cells involves cooperative fluctuations of segments of cell walls, attached proteins, and associated cytoplasmic proteins.

Computer simulations of the atomic mobilities of the component parts of crystalline and globular proteins have revealed extensive internal dynamics in the solid state at room temperature (Swaminathan et al., 1982; van Gunsteren & Karplus, 1982; Olejniczak et al., 1984; Karplus, 1987). Time-dependent determinations of the atomic Cartesian coordinates show that both main-chain and side-chain carbons and nitrogens have root-mean-square fluctuations of the order of 0.5 Å. Fluctuations in various protein dihedral angles are between 8 and 15°. Such internal rotational motions may have a role in the functions of some proteins (McCammon et al., 1979).

Experimental evidence for internal motions of this sort is available from temperature-dependent Debye–Waller factors of X-ray analysis of crystallizable proteins (Willis & Pryor, 1975; Northrup et al., 1980a,b; van Gunsteren & Karplus, 1982). In general, there is qualitative agreement between the extent of motion revealed by X-ray analysis and computer simulation of molecular dynamics. Differences may be due to contributions to the Debye–Waller factors from crystal disorder or to the limitation of the simulations to time scales shorter than 100 ps.

In this paper, we report the characterization by ^{15}N nuclear magnetic resonance (NMR)[1] of the mobility of proteins in intact lyophilized (10% water by weight) and wet cells (90% water by weight) of the bacterium *Aerococcus viridans* tagged with both specific and general ^{15}N labels. Since the static peptide dipolar NH coupling is known accurately, the diminution of this coupling by molecular motion (of frequency greater than the scaled NH 12-kHz coupling) is an unambiguous direct measure of protein mobility. The partial collapse by motion of the dipolar tensor can be measured in a dipolar rotational spin-echo ^{15}N NMR experiment (Munowitz & Griffin, 1982; Schaefer et al., 1983, Cross & Opella, 1985). The peptide ^{15}N chemical shift tensor is also partially averaged

†This work was supported, in part, by funds from NIH Grant GM40634.

[1] Abbreviations: NMR, nuclear magnetic resonance; CP, cross-polarization; MAS, magic-angle spinning; MREV-8, designation of a specific multiple-pulse homonuclear decoupling sequence; μ and ρ, chemical shift anisotropy parameters; θ, torsional angular excursion.

0006-2960/89/0428-1362$01.50/0

by the same molecular motion, and this averaging is reflected in the intensities of spinning side bands in slow-spinning magic-angle ^{15}N NMR experiments (Maricq & Waugh, 1979; Lewis et al., 1985).

Materials and Methods

Aerococcus viridans (*Gaffkya homari*). This bacterium was obtained from the American Type Culture Collection (ATCC 10400) and maintained on Difco tryptic soy broth at 30 °C. The synthetic medium (Miller & Evans, 1970) used in these experiments contained the following (in grams per liter): sodium glutamate, 5; D-glucose, 10; $(NH_4)_2SO_4$, 1.05; K_2HPO_4, 5; adenine, 5×10^{-3}; guanine, 5×10^{-3}; uracil, 5×10^{-3}; xanthine, 5×10^{-3}; biotin, 1×10^{-4}; folic acid, 1×10^{-5}; nicotinic acid, 2×10^{-3}; calcium pantothenate, 1×10^{-3}; pyridoxine hydrochloride, 2×10^{-3}; riboflavin, 1×10^{-3}; $MgSO_4 \cdot 7H_2O$, 0.2; $FeSO_4 \cdot 7H_2O$, 1×10^{-2}; and $MnSO_4 \cdot 4H_2O$, 1×10^{-2}. In addition, the medium contained 100 mg/L all 20 common L-amino acids. The pH of the medium was adjusted to 7.4–7.5 before use. In experiments involving [^{15}N]ammonium sulfate or [^{15}N]lysine, the labeled material directly replaced its natural-abundance counterpart.

Culture Method. An overnight culture of cells of *A. viridans* grown in 20 mL of tryptic soy broth medium was aseptically centrifuged at 7000*g* for 10 min, and the cellular sediment was used to inoculate 1 L of labeled synthetic medium contained in an Erlenmeyer flask. Growth with aeration and stirring was followed optically at 660 nm, and cells were harvested at an absorbance of 0.6 by centrifugation at 10000*g* for 10 min, washed once with 0.025 M potassium phosphate (pH 7.0), and centrifuged again. One liter of medium provided about 0.2 g of lyophilized cells.

Magic-Angle NMR. Cross-polarization magic-angle spinning ^{15}N NMR spectra were obtained at 20.3 MHz using matched spin-lock cross-polarization transfers with 2-ms single contacts and 35-kHz radio-frequency fields (Schaefer & Stejskal, 1979). Both lyophilized and wet samples were contained in a 700-μL Delrin hollow rotor, fitted with an o-ring seal, and spun using a double air-bearing system. Spectra were obtained from the collection of 50 000–100 000 scans with a repeat period of 1 s. Cells were maintained in the rotor at 10 °C by cooling the bearing and drive gas supplies. Spectra are presented with chemical shift scales in either hertz or ppm downfield from $(^{15}NH_4)_2SO_4$ as an external, solid reference material.

Dipolar Modulation. Dipolar rotational spin-echo ^{15}N NMR is a two-dimensional experiment in which, during the additional time dimension, the nitrogen magnetization generated by cross-polarization is allowed to evolve under the influence of N–H coupling while H–H coupling is suppressed by ^1H multiple-pulse irradiation (Munowitz & Griffin, 1982). For singly protonated peptide nitrogens whose resonances are well resolved in the chemical shift dimension, a Fourier transform of intensity at the peak maximum versus evolution time yields a dipolar spectrum consisting of a ^{15}N–^1H Pake doublet, scaled by the multiple-pulse decoupling, and broken up into side bands by magic-angle spinning required for high resolution in the solid state. This method has been discussed before (Schaefer et al., 1983) and illustrated by applications to the characterization of motion in solid glassy polymers (Schaefer et al., 1984a,b). In the latter applications, C–H dipolar coupling was observed, but the analytical techniques remain the same as used for the characterization of N–H coupling in proteins. Dipolar line shapes are similar to the more familiar ^2H quadrupolar NMR line shapes often used in the analysis of macromolecular systems (Spiess, 1983).

The H–H decoupling was achieved in the NH dipolar modulation experiment by a semiwindowless version (Burum et al., 1981) of the proton radio-frequency pulse sequence designated as MREV-8 (Haeberlen, 1976). This pulse sequence scales the heteronuclear N–H dipolar coupling by 0.536 (Burum et al., 1981). The length of the $\pi/2$ pulses of the sequence was 3.0 μs. The 33.6-μs cycle time of this sequence results in decoupling of proton–proton interactions as large as 60 kHz (1/16.8 μs) and was adjusted so that 16 cycles exactly fit in 1 rotor period (538 μs, corresponding to the spinning speed of 1859 Hz). Nitrogen dipolar tensor simulations were performed by using standard methods (Herzfeld & Berger, 1980). Calculations of tensors partially collapsed by restricted molecular motion were performed by assuming that the motion was fast compared to the dipolar interactions (Schaefer et al., 1984b).

Results

Lyophilized Cells. The refocusing of ^{15}N dipolar rotational spin-echoes is shown in Figure 1 for the sum of all uniformly ^{15}N-labeled proteins in intact lyophilized cells of *Aerococcus viridans*. The peptide–nitrogen resonance occurs at 95 ppm (from external ammonium sulfate) and is well clear of various side-chain nitrogen resonances (10–60 ppm), and of the minor spinning side bands arising from the mechanical sample spinning. Minor contributions to the 95 ppm signal arise from the side-chain amide nitrogens of asparagine and glutamine residues. After one rotor revolution, all NH vectors have been restored to the orientations they had at the beginning of the H–H irradiation period. Thus, all dephasing of nitrogen magnetization due to N–H coupling (illustrated in Figure 1 after 2, 4, and 8 MREV-8 cycles) has been refocused after a rotor period, and a dipolar rotational spin-echo results. The intensity of this echo should match that of the signal before any dephasing. The observed echo is 80% as intense (Figure 1, lower left), with losses due primarily to imperfect H–H decoupling.

A 16-point Fourier transform of the time-dependent modulation pattern traced out by the signal maximum at 95 ppm results in a dipolar side-band pattern broken into spinning side bands separated by the spinning speed for the average of all peptide NH's in the sample (Figure 1, top right). Each side band is represented by a single point in the dipolar frequency dimension. Intensities of the side bands can be reliably compared so long as side-band widths are all equal, an assumption we will make here.

The experimental dipolar side-band pattern does not agree with that calculated for a rigid NH spin pair (Figure 1, middle right) but does match a pattern calculated assuming the NH vector is undergoing restricted isotropic fluctuations on a sphere, with a root-mean-square angular excursion of 23° (Figure 1, bottom right). The experimental patterns for *A. viridans* specifically labeled with [α-^{15}N]lysine and [ϵ-^{15}N]-lysine, and the pattern for a crystalline glycylglycine derivative model peptide, are in similar agreement with the motionally averaged dipolar pattern (Table I). Lysine is incorporated without scrambling in *A. viridans*, so [α-^{15}N]lysine produces peptide NH exclusively. Fifty percent of the [ϵ-^{15}N]lysine appears in the peptidoglycan of cell walls, and half of that forms labeled D-Ala-L-Lys amide cross-links (Jacob et al., 1983). This means that all of the amide–nitrogen signal of [ϵ-^{15}N]lysine-labeled *A. viridans* arises from the cell wall (Figure 2).

Wet Cells. Cross-polarization magic-angle spinning ^{15}N NMR can also be used to detect labeled protein in viable wet cells of *A. viridans* (Figure 3). About half of the total lyo-

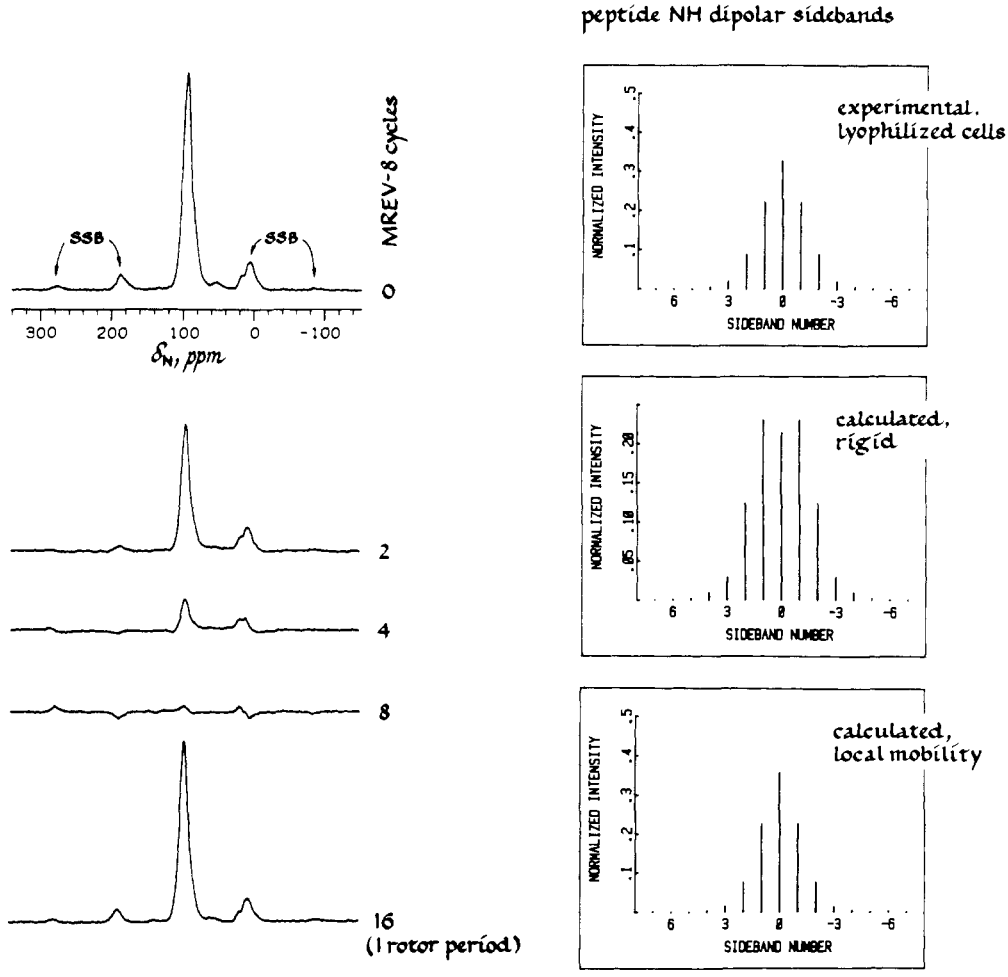

FIGURE 1: Dipolar rotational spin-echo 20.3-MHz ^{15}N NMR spectra (left) of ^{15}N uniformly labeled lyophilized intact cells of *A. viridans* at room temperature as a function of the number of semiwindowless MREV-8 cycles used during ^{1}H–^{15}N dipolar evolution. Magic-angle spinning was at 1859 Hz. Experimental and calculated dipolar patterns are shown at the right of the figure. The experimental pattern was the result of a 16-point Fourier transform of absorption mode data, examples of which are shown at the left.

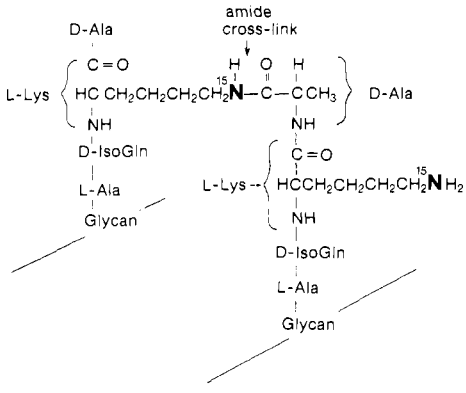

FIGURE 2: Cell wall peptidoglycan structure of *A. viridans* according to Nakel et al. (1971). Nitrogens shown in boldface are ^{15}N labeled using a medium containing L-[ϵ-^{15}N]lysine. One of the lysine groups is involved in a cross-link with an alanine from a separate peptide stem. IsoGln, isoglutamine residue.

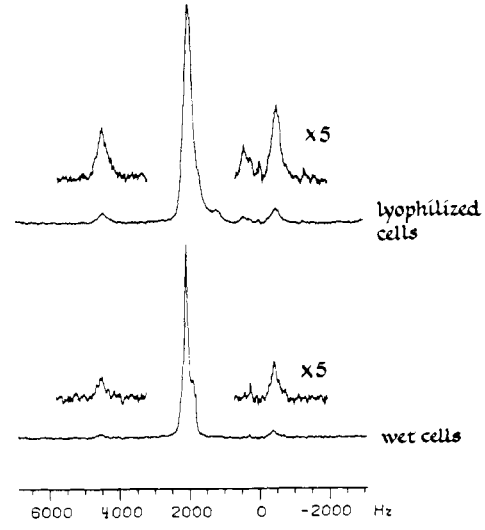

FIGURE 3: Cross-polarization magic-angle spinning 20.3-MHz ^{15}N NMR spectra of intact, viable cells of uniformly ^{15}N-labeled *A. viridans* before (bottom) and after (top) lyophilization. The vertical display scales have taken into account laboratory and rotating-frame relaxation times. Magic-angle spinning was at 2500 Hz. The external reference (0 Hz) is the ^{15}N resonance of solid ammonium sulfate.

philized cell integrated signal intensity is detected in a wet cell CPMAS experiment. Since we detected no solution-like main-chain protein signals in conventional FT NMR experiments (Shulman et al., 1979), we attribute the missing signal intensity to cells with large-amplitude motions having frequencies of the order of 100 kHz. Such motions are slow enough to interfere with line-narrowing solids NMR decoupling and not fast enough to average completely dipolar line broadening (Haeberlen & Waugh, 1968). Thus, cells, or parts of cells, undergoing these motions are simply not observed in either FT or CP experiments.

The wet cell spectrum of *A. viridans* (Figure 3, bottom) is a little better resolved than the corresponding lyophilized cell spectrum, and only a few side-chain ^{15}N signals have disap-

Table I: Dipolar Rotational Side-Band Intensities[a] for an NH Pair Undergoing Molecular Motion and Magic-Angle Spinning at 1859 Hz

expt or motional model	side-band no. 0	1	2	3	4	5	6
A. viridans, lyophilized intact cells, labeled by							
[α-^{15}N]lysine	0.345	0.217	0.083	0.016	0.006	0.002	0.003
[ϵ-^{15}N]lysine	0.334	0.215	0.089	0.019	0.001	0.000	0.003
[U-^{15}N]ammonium sulfate	0.327	0.222	0.089	0.019	0.005	0.001	0.000
$\phi CH_2OCONH^{13}CH_2{}^{13}CO$-$^{15}NHCH_2COOH$	0.340	0.215	0.091	0.018	0.004	0.001	0.000
calcd, rigid[b]	0.214	0.230	0.123	0.029	0.009	0.002	0.000
calcd, with local motion[c]	0.359	0.227	0.076	0.014	0.003	0.000	0.000

[a] Semiwindowless MREV multiple-pulse decoupling. Theoretical scale factor is 0.54. [b] N–H bond length is 1.01 Å (Verbist et al., 1972); scaled N–H dipolar coupling is 11.819 kHz. [c] Restricted isotropic motion on a sphere; rms angular fluctuations of 23°. The mean was taken of the square of the sines of the angles rather than the squares of the angles themselves to obtain a root-mean-square.

Table II: Chemical Shift Rotational Side-Band Intensities[a] for Some Amide Nitrogens

expt or motional model	side-band no. 2	1	0	−1	−2
A. viridans, lyophilized intact cells, labeled by					
[U-^{15}N]ammonium sulfate	0.070	0.137	0.453	0.278	*c*
[ϵ-^{15}N]lysine[b]	0.091	0.152	0.485	0.273	*c*
A. viridans, viable wet cells labeled by					
[U-^{15}N]ammonium sulfate	0.034	0.080	0.721	0.144	0.021
[ϵ-^{15}N]lysine	0	0.057	0.786	0.157	0
calcd, rigid[d]	0.128	0.122	0.285	0.350	0.066
calcd, with local motion[e]	0.085	0.133	0.450	0.282	0.030
calcd, with increased motions[f]	0.026	0.080	0.766	0.118	0.008

[a] Larmor frequency of 20.3 MHz and magic-angle spinning at 930 Hz. [b] The [ϵ-^{15}N]lysine incorporated into cell walls results in an [^{15}N]amide–peptidoglycan cross-link. [c] The high-field second-spinning side band was obscured by a strong amino[^{15}N]lysine peak. [d] $\mu = 4.5$ and $\rho = 1.0$, where $\mu = \omega_{33} = \omega_{11}$, $\rho\mu = 3\omega_{22}$, and $\omega_{33} \geq \omega_{22} \geq \omega_{11}$ (Schaefer et al., 1984b). [e] Restricted isotropic motion on a sphere; rms angular fluctuations of 22.6°; $\mu = 3.5$, $\rho = 1.0$. [f] Restricted isotropic motion on a sphere; rms angular fluctuations of 37.5°; $\mu = 2.0$, $\rho = 1.0$.

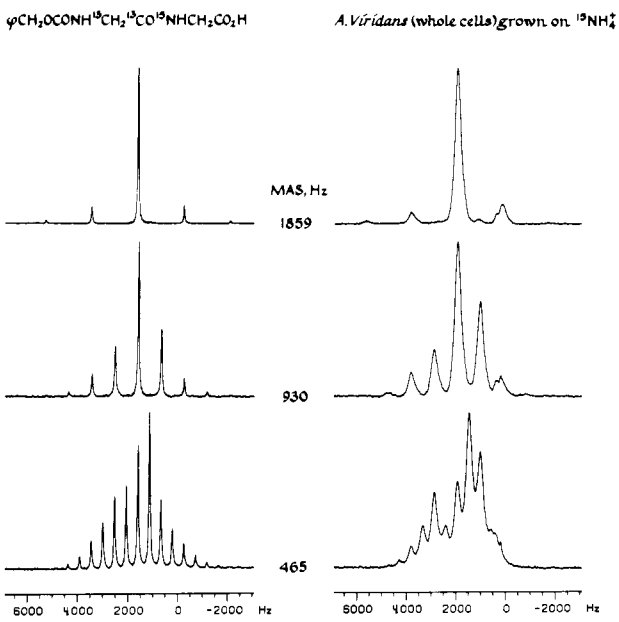

FIGURE 4: Cross-polarization 20.3-MHz ^{15}N NMR spectra of a glycylglycine derivative crystalline model compound (left) and of intact lyophilized cells of uniformly ^{15}N-labeled *A. viridans* (right) for three different magic-angle spinning speeds.

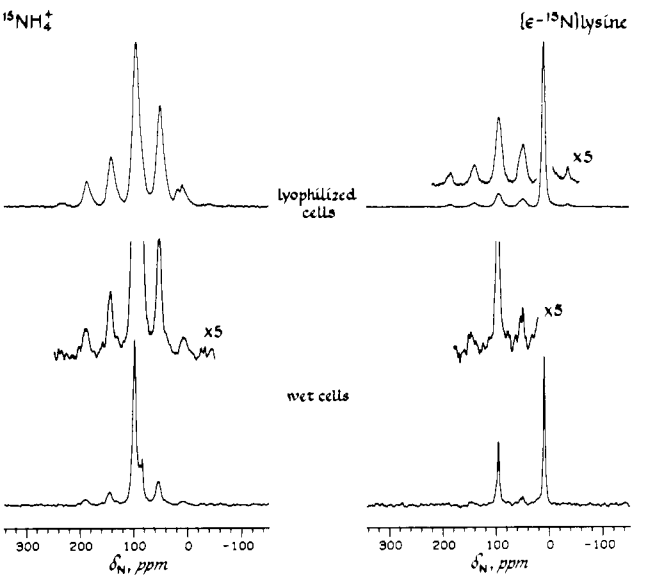

FIGURE 5: Cross-polarization magic-angle spinning 20.3-MHz ^{15}N NMR spectra of intact lyophilized cells (top) and viable wet cells (bottom) of *A. viridans* uniformly ^{15}N labeled (left) and specifically labeled by [ϵ-^{15}N]lysine (right). Magic-angle spinning was at 930 Hz. Both the center band and spinning side bands are narrower in the spectra of the wet cells than in those of the lyophilized cells. The amide–nitrogen signal (centered at about 100 ppm) of the [ϵ-^{15}N]-lysine-labeled *A. viridans* arises exclusively from the cell wall (Figure 2). The absolute vertical display scales of the spectra on the right differ from those on the left. The relative vertical display scales comparing lyophilized cell (top) and wet cell spectra (bottom) with the same ^{15}N label have taken into account laboratory and rotating frame relaxation times.

peared (25 and 60 ppm, 500 and 1200 Hz, respectively, from zero reference). However, rotational spin-echo refocusing was substantially decreased because of increased homogeneous relaxation in the wet cell systems. This lowered sensitivity, and so made impractical full two-dimensional dipolar modulation experiments. Thus, dipolar side-band intensities for wet cell samples are not reported in Table I.

The main-chain peptide–nitrogen chemical shift spinning side bands in one-dimensional CPMAS spectra appear only about half as intense relative to the center band (Figure 3). This suggests additional motional averaging of the main-chain peptide–nitrogen chemical shift tensors in the wet cells. A quantitative assessment of this motional averaging is best carried out at low spinning speed, where spinning side bands are intense. A magic-angle spinning speed of 930 Hz results in strong spinning side bands which are well resolved, even in the spectrum of the lyophilized intact cells (Figure 4). The intensities of the amide–nitrogen chemical shift anisotropies

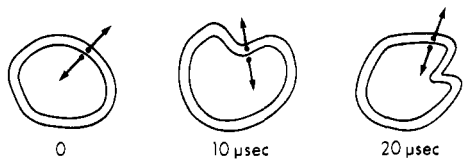

FIGURE 6: Schematic drawing of a possible 100-kHz motion of a bacterial cell which involves cooperative fluctuations of segments of cell walls, attached proteins, and associated cytoplasmic proteins.

both for general protein in *A. viridans* and for peptidoglycan cross-links are about the same in lyophilized intact cells (Figure 5, top, and Table II, rows 1 and 2). These spectra indicate static chemical shift anisotropy parameters of $\mu = 4.5$ and $\rho = 1.0$ (Schaefer, 1984b), reduced by the motion detected in the lyophilized cell dipolar modulation experiment to $\mu = 3.5$ and $\rho = 1.0$ (Table II, row 6). The corresponding parameters for the wet cells are further reduced by additional restricted isotropic motion to $\mu = 2.0$ and $\rho = 1.0$ (Figure 5, bottom, and Table II, rows 3, 4, and 7). Both the general protein and cell wall peptidoglycan wet cell amide–nitrogen chemical shift anisotropies are motionally averaged to the same extent.

Discussion

Local Motions in Solids. The widths of the dipolar side-band patterns for both general and specific amide labels in lyophilized intact cells of *A. viridans* are substantially narrower than those expected for a genuinely rigid material. This is also true for the dipolar pattern of the nominally rigid glycyl peptide crystalline model compound (Table I). The reduction in dipolar coupling is due to ultra-high-frequency motional averaging (Schaefer et al., 1983). As much as half of the averaging of ^1H–^{15}N dipolar coupling can be attributed to temperature-independent, internal mode, bond vibrational motion (Henry & Szabo, 1985). The remainder is due to rigid-body, temperature-dependent, external-mode, rotational motion (Dunitz et al., 1988). The latter includes the angular reorientations and librations commonly observed in computer simulations of the dynamics of the interiors of globular proteins (Karplus, 1987). Neither mode of motion is highly molecule specific (van Gunsteren & Karplus, 1982; Henry & Szabo, 1985), and the net averaging of the ^1H–^{15}N dipolar coupling is equivalent to that of fast, restricted isotropic motion with an angular excursion from equilibrium defined by an rms fluctuation angle, θ. The extent of averaging of the dipolar coupling is then given by the factor $1 - 3 \sin^2 \theta/2$ (Schaefer et al., 1984b).

We observe an NH vector rms angular excursion of 23° (Table I, row 6), about half of which, or 12°, we attribute to rigid-body rotational motions (Dixon et al., 1988). The rms dihedral angular fluctuation for the peptide main chain of bovine pancreatic trypsin inhibitor is 8° in dynamic simulations (van Gunsteren & Karplus, 1982). Since some of the motions of the C_α–C and N–C_α pairs of the main-chain dihedral angle fluctuations are correlated (which reduces the net dihedral angle excursion), a slightly larger value for the NH vector rigid-body angular excursion by itself is expected. The simulations show that these local motions occur throughout the interiors of proteins and that anisotropies in the motions are relatively small. Thus, the motions can be reasonably well described by the restricted isotropic motional model employed for the calculations of Table I. The average restricted isotropic main-chain excursion for protein in *A. viridans* is comparable to that reported for main-chain rotations about the draw axis of specifically labeled collagen fibers. The latter have been established from the partial collapse of chemical shift tensors (Jelinski & Torchia, 1980; Sarkar et al., 1985).

The spinning side-band patterns of the chemical shift tensors for lyophilized cells of *A. viridans* uniformly ^{15}N labeled, and labeled by [ϵ-^{15}N]lysine, also reflect the averaging of ultra-high-frequency motions. Thus, the center bands of the experimental rotational side-band patterns are greater than either the upper or the lower first side band (Table II, rows 1 and 2), while the center bands expected for totally rigid patterns are less than the upper first spinning side band (Table II, row 5). The lyophilized whole cell spectra show no evidence of additional averaging of the amide–nitrogen chemical shift tensor by slower, large-amplitude motions. This conclusion is based on the fact that the chemical shift side-band pattern for the uniformly ^{15}N-labeled cells has the same shape as that of the glycyl peptide crystalline model compound (Figure 4), for which slow motions are absent.

Motions in Wet Cells. The whole cell chemical shift side-band patterns are considerably averaged in the viable wet state. The center bands for the wet cell patterns represent about 75% of the total intensity, compared to less than 50% of the lyophilized cell patterns (Figure 5). This averaging can be accounted for by increasing the sector of the sphere on which a peptide– or amide–NH vector is undergoing restricted isotropic excursions from 23° to 37° (Table II, row 7). Since both general peptide NH and cross-linked cell wall peptidoglycan–amide NH are averaged to the same extent, the responsible motion is necessarily general, or global. Assuming an isolated whole cell rotates 90° in 100 ms (Berg & Brown, 1972), we can expect a 45° rms excursion in 25 ms. However, 45° excursions in 0.2 ms are needed to account for the observed averaging of the chemical shift anisotropy. In addition, *A. viridans* is not motile and is unlikely to undergo significant whole cell rotations of any sort in the dense packing present in wet cell magic-angle spinning. Finally, the wet cell spectrum was obtained under cross-polarization conditions which rules out full isotropic rotational reorientation on a millisecond time scale.

The observed averaging may arise, at least in part, from cooperative reorientational dynamic fluctuations which involve segments of cell wells, attached proteins, and associated cytoplasmic proteins (Figure 6). Such cooperative large-scale motions are found in plasticized, multiphase, solid synthetic polymers (Schaefer et al., 1987), although their description on the molecular scale is often incomplete. The frequencies of such motions likely extend from 10 kHz up to the low-megahertz regime. We known that some 100-kHz motions are present because of the interference with dipolar decoupling and resulting incomplete detection of part of the wet cell signal. Motions in the 10-kHz to 10-MHz regime have not been accounted for by the computer simulations of molecular dynamics in proteins performed to date. Such motions, however, have been invoked to account for the self-propulsion of whole cells when viewed as swimmers in a fluid medium (Shapere & Wilczek, 1987).

Registry No. $\phi CH_2OCONH^{13}CH_2{}^{13}CO^{15}NHCH_2CO_2H$, 80058-04-4.

References

Berg, H. C., & Brown, D. A. (1972) *Nature (London) 239*, 500–504.

Burum, D. P., Linder, M., & Ernst, R. R. (1981) *J. Magn. Reson. 44*, 173–188.

Cross, T. A., & Opella, S. J. (1985) *J. Mol. Biol. 182*, 367–381.

Dixon, W. T., Keller, R., Conradi, M. S., & Schaefer, J. (1988) *J. Magn. Reson.* (submitted for publication).

Dunitz, J. D., Schomaker, V., & Trueblood, K. N. (1988) *J. Phys. Chem. 92*, 856–867.
Greenfield, M. S., Vold, R. L., & Vold, R. R. (1985) *J. Chem. Phys. 83*, 1440–1443.
Haeberlen, U. (1976) *High-Resolution NMR in Solids, Selective Averaging*, pp 92–98, Academic, New York.
Haeberlen, U., & Waugh, J. S. (1968) *Phys. Rev. 175*, 453–467.
Henry, E. R., & Szabo, A. (1985) *J. Chem. Phys. 82*, 4753–4761.
Herzfeld, J., & Berger, A. E. (1980) *J. Chem. Phys. 73*, 6021–6030.
Jacob, G. S., Schaefer, J., & Wilson, G. E., Jr. (1983) *J. Biol. Chem. 258*, 10824–10826.
Jelinski, L. W., & Torchia, D. A. (1980) *J. Mol. Biol. 138*, 255–272.
Karplus, M. (1987) *Phys. Today*, 68–72.
Koetzle, T. F., Lehman, M. S., & Hamilton, W. C. (1973) *Acta Crystallogr., Sect. B: Struct. Crystallogr. Cryst. Chem. B29*, 231–236.
Lewis, B. A., Harbison, G. S., Herzfeld, J., & Griffin, R. G. (1985) *Biochemistry 24*, 4671–4679.
Maricq, M., & Waugh, J. S. (1979) *J. Chem. Phys. 70*, 3300–3316.
McCammon, J. A. (1984) *Rep. Prog. Phys. 47*, 1–46.
McCammon, J. A., Wolynes, P. G., & Karplus, M. (1979) *Biochemistry 18*, 927–942.
Miller, T. L., & Evans, J. B. (1970) *J. Gen. Microbiol. 61*, 131–135.
Munowitz, M. G., & Griffin, R. G. (1982) *J. Chem. Phys. 76*, 2848–2858.
Nakel, M., Ghuysen, J. M., & Kandler, O. (1971) *Biochemistry 10*, 2170–2175.
Northrup, S. H., Pear, M. R., McCammon, J. A., & Karplus, M. (1980a) *Nature (London) 286*, 304–305.
Northrup, S. H., Pear, M. R., McCammon, J. A., Karplus, M., & Takano, T. (1980b) *Nature (London) 287*, 659–660.
Olejniczak, E. T., Dobson, C. M., Karplus, M., & Levy, R. M. (1984) *J. Am. Chem. Soc. 106*, 1923–1930.
Sarkar, S. K., Sullivan, C. E., & Torchia, D. A. (1985) *Biochemistry 24*, 2348–2354.
Schaefer, J., & Stejskal, E. O. (1979) in *Carbon-13 NMR Spectroscopy* (Levy, G. C., Ed.) Vol. 3, pp 284–324, Wiley, New York.
Schaefer, J., McKay, R. A., Stejskal, E. O., & Dixon, W. T. (1983) *J. Magn. Reson. 52*, 123–129.
Schaefer, J., Sefcik, M. D., Stejskal, E. O., McKay, R. A., Dixon, W. T., & Cais, R. E. (1984a) *Macromolecules 17*, 1107–1118.
Schaefer, J., Stejskal, E. O., McKay, R. A., & Dixon, W. T. (1984b) *Macromolecules 17*, 1479–1489.
Schaefer, J., Garbow, J. R., Stejskal, E. O., & Lefelar, J. A. (1987) *Macromolecules 20*, 1271–1278.
Shapere, A., & Wilczek, F. (1987) *Phys. Rev. Lett. 58*, 2051–2054.
Shulman, R. G., Brown, T. R., Ugurbil, K., Ogawa, S., Cohen, S. M., & den Hollander, J. A. (1979) *Science (Washington, D.C.) 205*, 160–166.
Spiess, H. W. (1983) *Colloid Polym. Sci. 261*, 193–209.
Swaminathan, S., Ichieye, T., van Gunsteren, W. F., & Karplus, M. (1982) *Biochemistry 21*, 5230–5241.
van Gunsteren, W. F., & Karplus, M. (1982) *Biochemistry 21*, 2259–2274.
Verbist, J. J., Lehmann, M. S., Koetzle, T. F., & Hamilton, W. C. (1972) *Acta Crystallogr., Sect. B: Struct. Crystallogr. Cryst. Chem. B28*, 3006–3013.
Willis, B. T. M., & Pryor, A. W. (1975) *Thermal Vibrations in Crystallography*, Chapter 6, Cambridge University Press, Cambridge, U.K.